

Structure formation of TiB₂-TiC-B₄C-C hetero-modulus ceramics via reaction hot pressing

O. Popov¹, S. Chornobuk^{1,2}, V. Vishnyakov³

¹Faculty of Physics, Taras Shevchenko National University of Kyiv, 4 Hlushkov Ave., Kiev 03187, Ukraine

²Science and Research Centre “Synthesis”, Kiev 02139, Ukraine

³Materials Research Institute, University of Huddersfield, HD1 3DH, UK

Abstract.

The densification kinetics and structure of TiB₂-TiC-C, TiB₂-C and TiB₂-B₄C-C hetero-modulus ceramics produced via reaction hot-pressing of B₄C and TiC precursors are investigated. The reaction begins at 1100°C with boron carbide decomposition and progresses in two main stages which can be predominantly determined by the boron atoms to TiC grains diffusion mechanisms. The solid phase grain boundary diffusion starts at 1100°C and effective gas phase transport finalises the reaction at temperatures above 1400°C. Two distinctive waves of the charge consolidation allow densifying investigated refractory materials at 1900°C and 30MPa during 16 minutes. The reaction is shown to define the features of the composite structure: submicron TiB₂ particles and faceted voids in B₄C matrix, flake-like graphite and TiB₂ inclusions in TiC matrix. High concentration of carbon atoms (~ 10 at.%) in synthesized diboride titanium grains have been observed.

Keywords: hetero-modulus ceramics, structure, reaction hot pressing, interaction mechanisms, densification

1. Introduction

Anoxic ceramics possess excellent properties such as high melting points, hardness and Young's modulus [1] which make it possible to use them as structural materials under extreme conditions of ultrahigh temperature [2, 3]. The main issue for all materials based on covalent bonding structure is their brittleness which results in low toughness and low thermal stress resistance [4]. This also adds to poor machinability [5] and limit practical use of such materials. Hasselman with coworkers managed to improve thermal shock durability of alumina [6] and zirconium carbide [7] by adding h-BN (hexagonal boron nitride) and experimentally confirmed [4] that the thermal stress resistance of ceramics with high values of Young's modulus can be increased considerably by the adding “soft” dispersed phase particles. Similarly, low-E (where E is Young's modulus) inclusions of graphite or graphite-like boron nitride can also improve machinability and oxidation stability of such superhard materials as silicon nitride [5, 8], boron carbide [9], transitional metals carbides [10 – 12]. The term “Hetero-Modulus Ceramics” (HMC) is slowly established in

the ceramic community. It is worth to note that mentioned above HM gained machinability and thermal shock resistance, inevitably lost hardness but their high temperature characteristics have not degraded as both boron nitride and graphite melting points are higher than 3000°C [13].

It is possible to anticipate that the toughness and strength would decrease with “soft” phase fraction inclusion which indeed has been shown experimentally for h-BN-containing HMC with various matrixes such as B₄C [9], ZrC [7], Al₂O₃ [6] and Si₃N₄ [5]. Nevertheless, there are some data in the similar composites showing strength [8] or toughness [14] rise at 5 – 10 vol. % of soft phase. The only substantial difference of the latter set of ceramics was that the nanoscale sizes of boron nitride inclusions they contained. On this basis it is possible to predict that one, by the providing proper composite dispersion, can improve both machinability and toughness.

Ceramic sintering temperature depends to the great extent on the initial powder melting point, so it is expectable that anoxic HMC sintering process requires heating to ultrahigh temperatures. For example TiC-graphite composites were hot pressed at 2700°C for 30 minutes [10]. Enthalpy of the reactions can aid with the lowering sintering temperature and the authors [15] managed to optimize TiC-TiB₂-C composite sintering conditions to 1900°C and 16 minutes using the reaction between TiC and B₄C during charge consolidation. Fracture toughness of sintered composites has depended strongly on graphite inclusion content having maximum at 5 – 15 vol. % of the soft phase. The possibility of such improvement have been claimed to be connected to the peculiarities of the composite structure which was developed via aforementioned solid phase reaction. However both reaction and structure were described just in outline.

The main purpose of the present work is to investigate TiC-B₄C reactions and synthesis parameters influence on consolidation kinetics and structure of TiC-TiB₂-C and B₄C-TiB₂-C HMCs.

2. Experimental

Commercially available powders of TiC (30 – 50 μm) and B₄C (60 μm) (all of them produced by Donetsk Reactive Factory, Ukraine) were used as starting materials. Both materials have 99.0% purity.

2.1. Bulk ceramic sample sintering and preparation

The powder mixtures of different compositions (Table 1) were grinded in a planetary mill for 16 minutes and hot-pressed in a graphite die, without a special protective atmosphere. Hot-pressing temperatures ranged from 1800 to 1950 °C for main sample set (№1 - №10) and from 1200 to 1800 °C for additional one (№11 - №13). The pressure of 30 MPa and isothermal dwelling time of 16 minutes were applied for hot-pressing procedure. Densification kinetics was observed during the hot-pressing using video registration of micrometre with an error of not more than 10 μm.

Table 1.

Initial powder composition and sintering temperature

№	TiC, at. %	B ₄ C, at. %	Sintering temperature, °C
1	4.3	95.7	1900
2	7.4	92.6	1850
3	13.8	86.2	1800
4	21	79	1800
5	28.5	71.5	1800
6	44.4	55.6	1800
7	61.5	48.5	1850
8	76.2	23.8	1900
9	86.5	13.5	1900
10	93.2	6.8	1950
11	44.4	55.6	1200
12	44.4	55.6	1400
13	44.4	55.6	1600

The bulk densities of obtained materials were measured using the Archimede's method and relative densities were calculated on the basis of the theoretical densities of TiB₂ (4.495 g/cm³), TiC (4.9 g/cm³), B₄C (2.51 g/cm³) and C (graphite) (2.28 g/cm³) assuming the rule of mixtures. Crystalline phase presence in the hot-pressed specimens was determined by X-ray diffractometry (DRON-4M, St. Petersburg, Russia). Microstructural observations and local compositional analysis measurements were taken with SEM and SEM-EDX. For further investigation, some specimen surfaces were polished with diamond abrasive powders. The heat effect and adiabatic temperature were calculated using thermochemistry data from the NIST Chemistry WebBook [10].

2.2. Contactless investigation of the interaction between TiC and B₄C

To clarify the influence of B₄C decomposition on TiB₂ formation mechanisms the possibility of contactless interaction (gas phase transport) between titanium and boron carbides at 1100 – 1900 °C was investigated in a separate set of experiments.

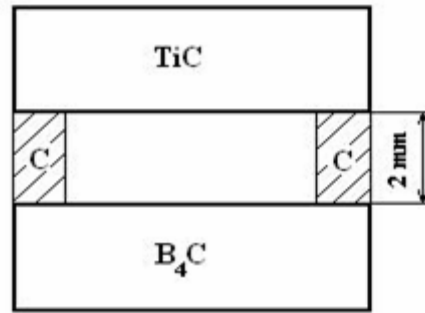


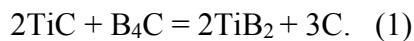
Figure 1. Contactless interaction experiment package drawing

For this purpose TiC and B₄C discs (d = 10mm, h = 5mm) from pure materials were sintered at 1300°C and 10MPa for 16 minutes and had relative density of approximately 60%. Sample surfaces were grinded and cleaned with acetone. Graphite ring was positioned between titanium and boron carbide plates to prevent contact (Fig.1). The package was annealed in graphite die for 16 minutes with no special protective atmosphere. This way, the time and atmosphere were similar to those of main samples (№ 1 – 10, Table 1) sintering. Phase changes of both surfaces after annealing were investigated with XRD.

3. Results and discussion

3.1. Densification and new phase emerging

The X-ray diffractometry of hot-pressed ceramics presented in Fig.2 has showed that the sintering process causes the initial TiC and B₄C phase content reduction and this has been coincided with TiB₂ and graphite formation. It was proposed by us earlier that the following chemical reaction between titanium and boron carbides in this case takes place:



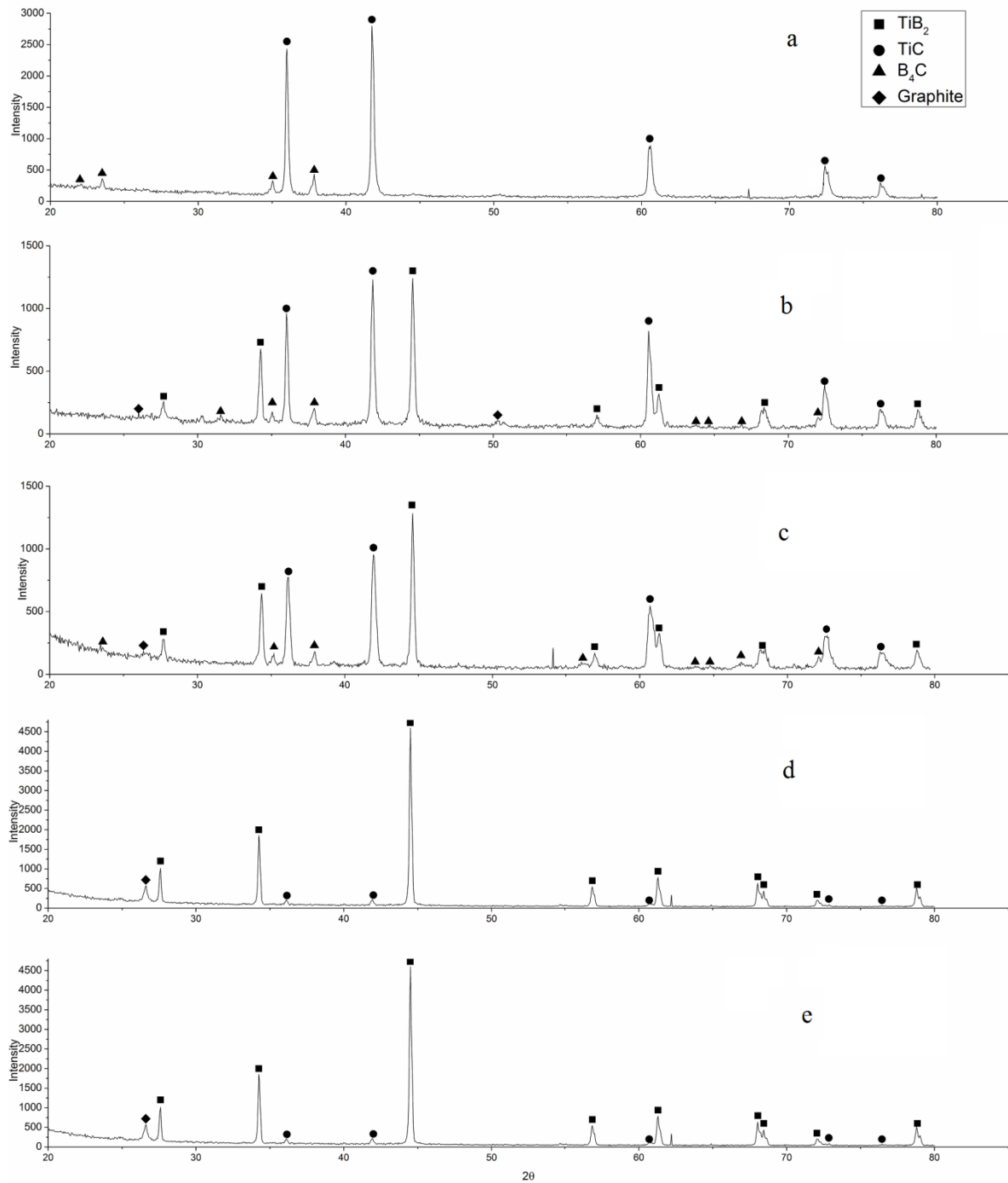


Figure 2. X-ray diffractometry of stoichiometric ($2\text{TiC-B}_4\text{C}$) composition (samples 6, 11-13, Tab.1) sintered at different temperatures: *a* – initial powder; *b* – 1200°C ; *c* – 1400°C ; *d* – 1600°C ; *e* – 1800°C .

As it can also be seen in Fig.2, the reaction (1) begins at a temperature which is lower than 1200°C and progresses slowly up to 1400°C . Further increases in temperature lead to considerable reaction rate rising, so it is mostly completed after 16 minutes at 1600°C (Fig.2d).

Table 2.

Composition (estimated considering reaction 1 to be completed [8]) and density of the samples after hot pressing

№	TiC, v. %	B ₄ C, v. %	TiB ₂ , v. %	C, v. %	ρ, g/cm ³	ρ ^{theor} , g/cm ³
1	0	89.7	6.8	3.5	2.64	2.65
2	0	82.2	11.8	6	2.79	2.75
3	0	67.3	21.6	11.1	3.12	2.95
4	0	50.7	32.6	16.7	3.4	3.16
5	0	33.9	43.7	22.4	3.64	3.37
6	1	0	65	34	4.15	3.77
7	34.5	0	43.3	22.2	4.41	4.16
8	61.2	0	25.6	13.2	4.72	4.46
9	78.7	0	14.1	7.2	4.83	4.66
10	89.4	0	7	3.6	4.79	4.78

G
raphics
in Fig.3
illustrat
e the
differen

ces in densification kinetics of samples 2, 6 and 9 (Tab.2). In sample 6 (Fig. 3b) the first stage of significant porosity decreasing begins at 1100°C and the second one at 1550°C. Considering Fig.2 these stages correspond to the beginning of the reaction (1) below 1200°C and its acceleration between 1400°C and 1600°C, so they should be the reflections of different interaction mechanisms.

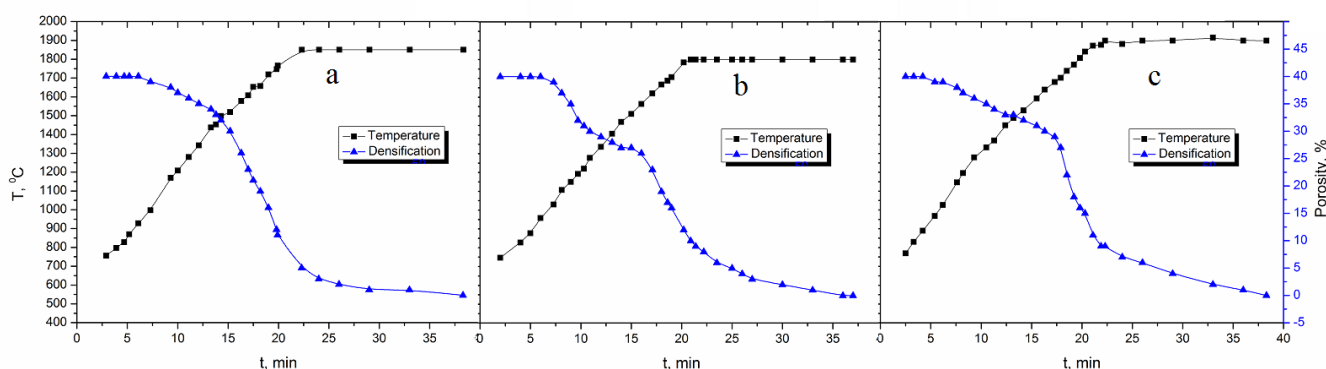


Figure 3. Densification kinetics for samples: №2 (a), №6 (b) and №9 (c).

Similar stages in relevant temperature intervals can be seen in Fig. 3a and 3c though they are not so clear. The latter proves the reaction process affects the densification as samples 2 and 9 initial powders contain no more than 20% of stoichiometric (2TiC-B₄C, equation 1) mixture while the 6-th sample titanium to boron carbides ratio is just 2:1 (see Table 1). There is one more simply noted attribute of the sintered samples: densities of the composites are higher than corresponding theoretical values and the discrepancy is again the greatest (~ 10%) for the stoichiometric composition (See Table 2). The mismatch is striking because the reaction (1) occurs with no dilatometric effect: the densities of 2TiC+B₄C and 2TiB₂+3C compositions differ not more than 0.1%. It means that the deviation cannot be explained just with the completeness of the transformation (actually noticeable in Fig. 1 as very little but distinct TiC peaks).

3.2. Structure of the composites

Phase distribution on composite fracture surfaces presented in Fig. 4 – 6 corresponds to XRD data [15] and reflects phase composition variation according to initial component ratio. Low TiC in initial powder content, like in samples 2 and 4 (Fig. 4, 7a) provides boron carbide matrix with titanium diboride and graphite inclusions.

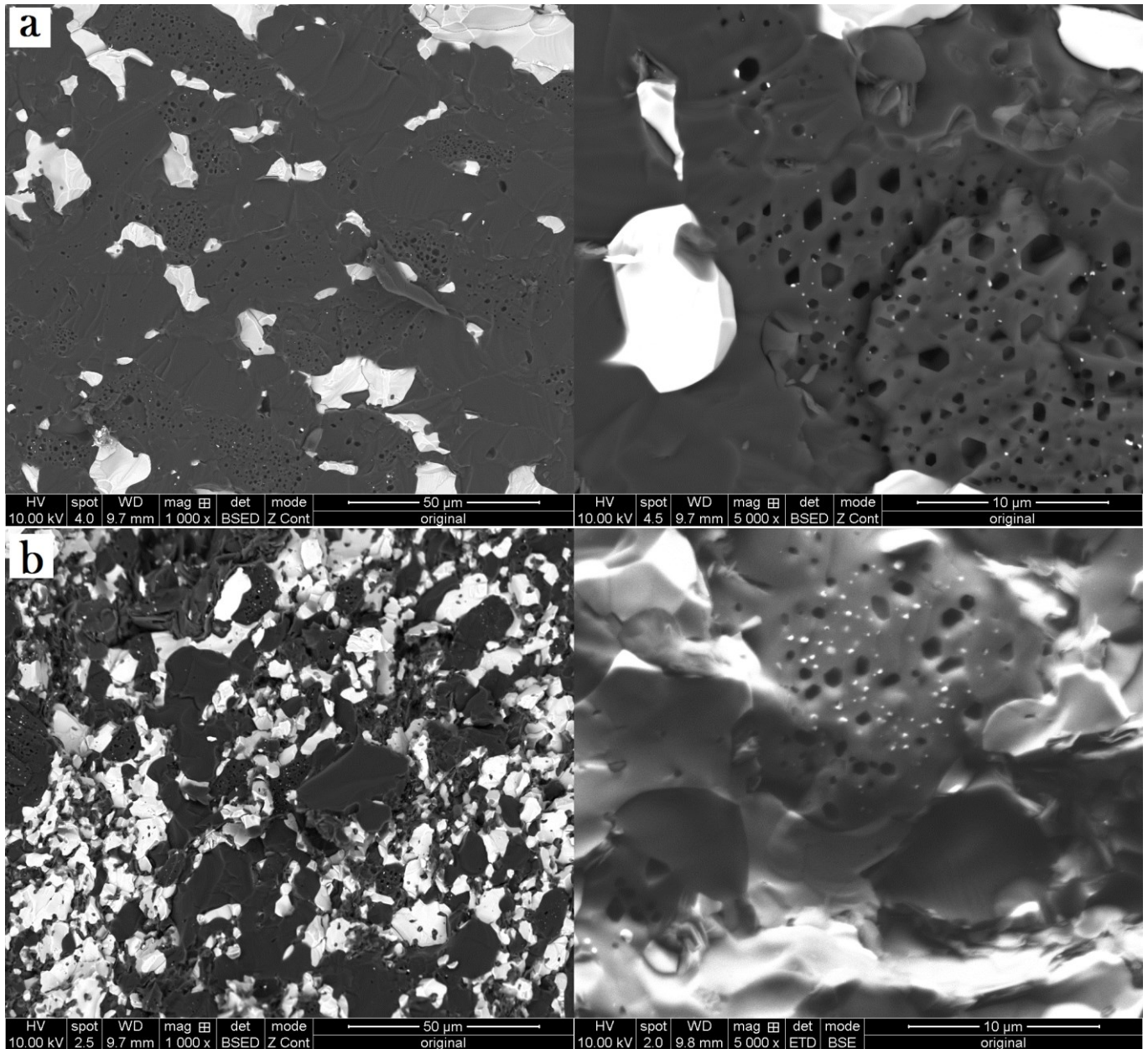


Figure 4. SEM analysis of sintered sample fracture surfaces: No2 (a), No4 (b)

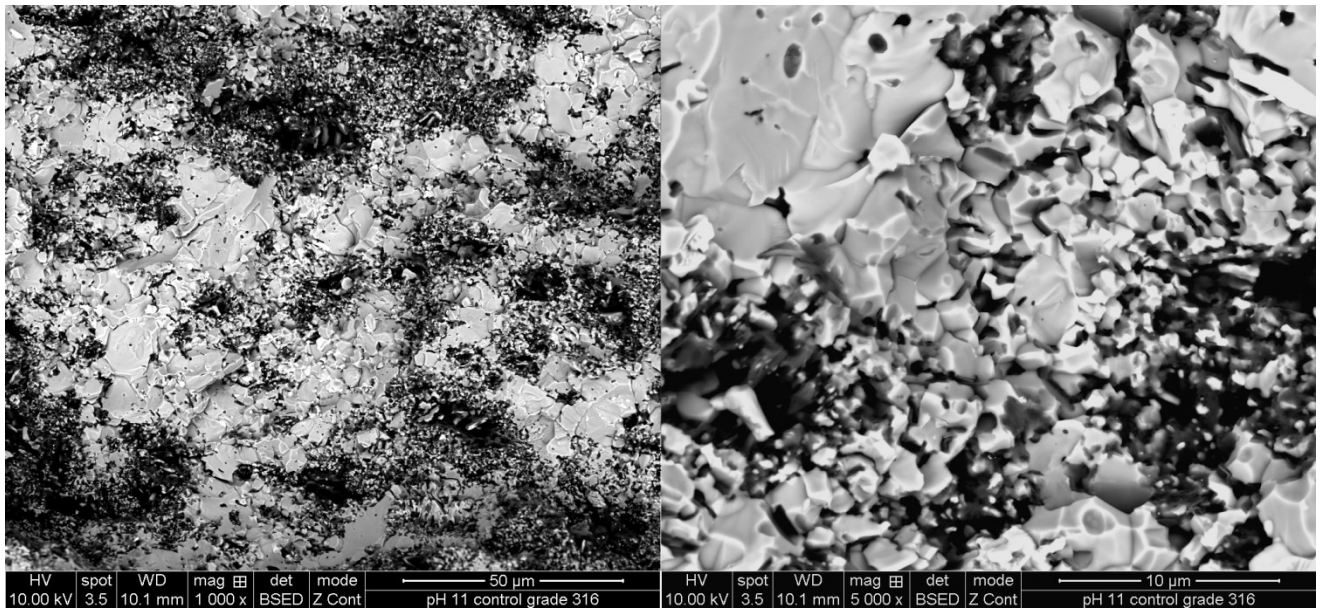


Figure 5. SEM analysis of sintered sample 6 fracture surface

Boron and titanium carbides disappearance during hot pressing of stoichiometric mixture (sample 6, Tables 1, 2) leads to formation of TiB_2 -based matrix containing considerable, up to 34 vol.% amount of carbon precipitates (Fig. 5). Further initial TiC content increasing (samples 7 – 10, Table 1, Fig. 6) results

similar composites with titanium carbide and diboride matrix.

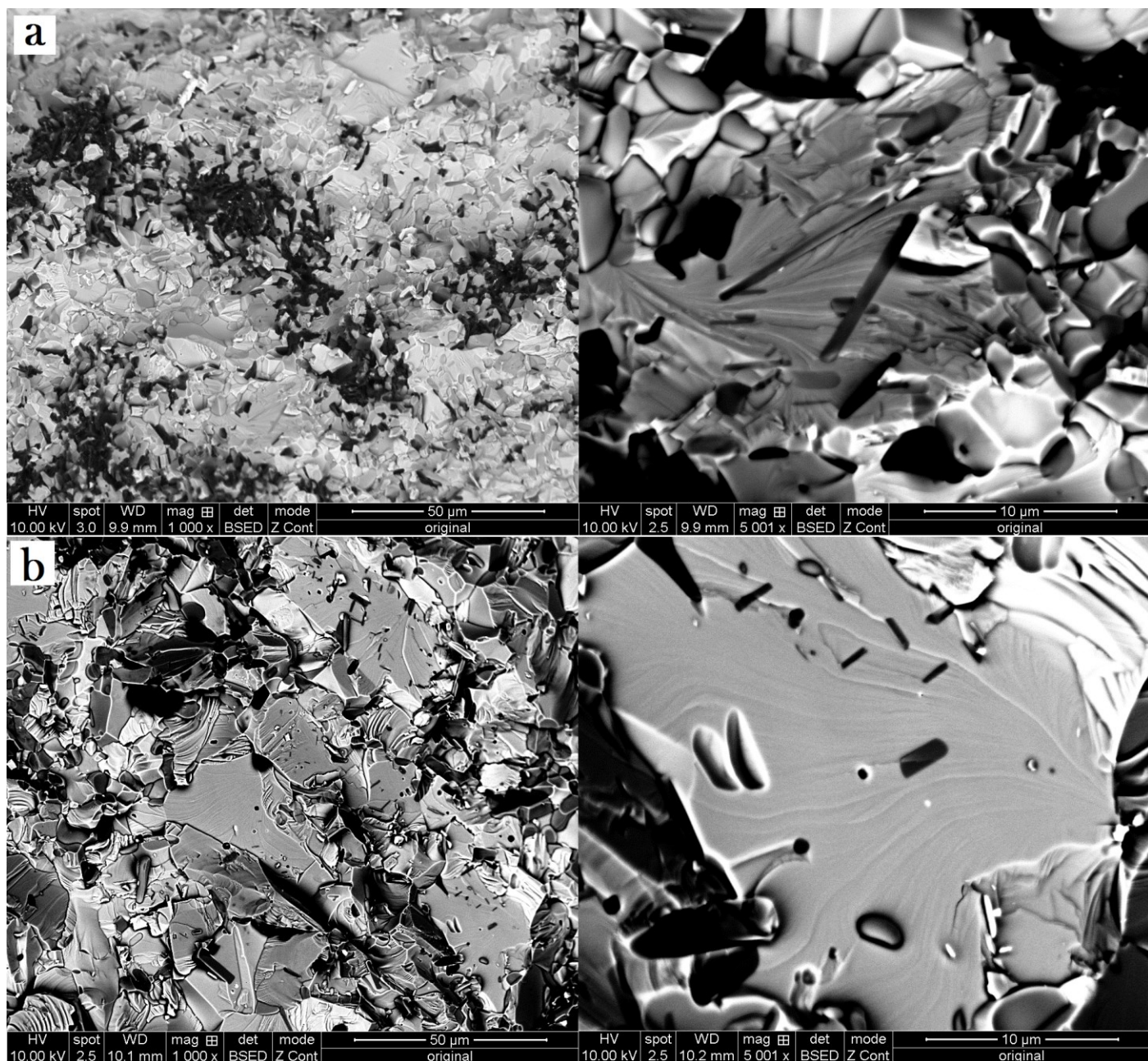


Figure 6. SEM analysis of sintered sample fracture surfaces: №7 (a), №9 (b)

Analysis of SEM pictures (Fig. 4 – 6) allows noting some features of sintered materials structure. Boron carbide matrix of samples 1 – 5 (see Fig. 4) contains certain amount of micro voids bordered with smooth walls resembling crystalline faceting. Considering that the walls of different voids within the same grain are parallel to each other one can definitely connect them to boron carbide crystal plains. Another peculiarity of mentioned samples is two types of titanium diboride grains: crystallites of 2 – 10 μm and submicron inclusions allocated within boron carbide matrix. It is evidently that relatively large grains inherit initial powder structure while submicron particles (Fig. 4) within B₄C crystals should reflect sintering process peculiarities. Diboride particles in the samples 7 – 10 (Table 1, Fig. 6) are also of two different

types: shapeless grains alternated with graphite and plate-like ones surrounded by TiC.

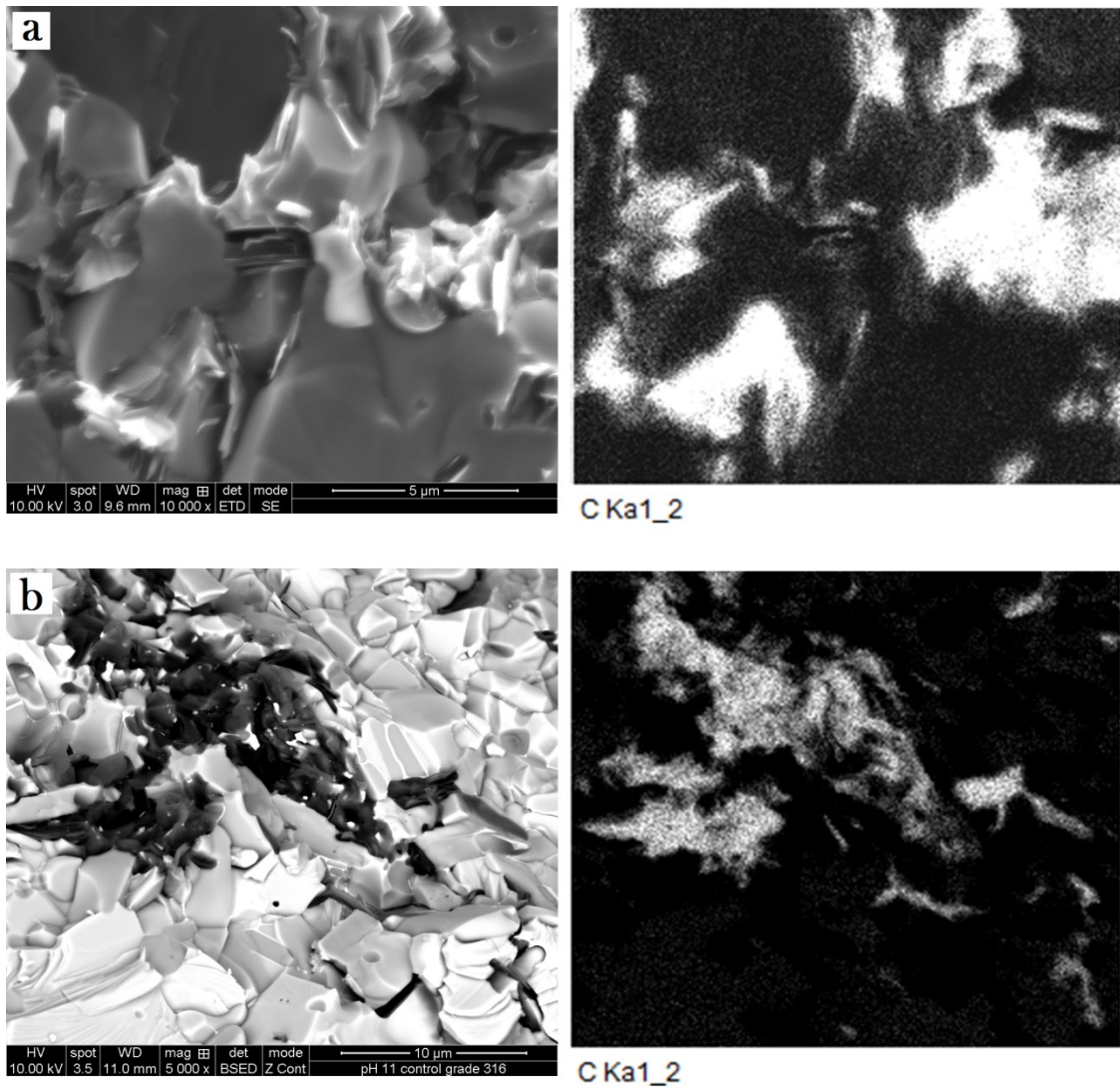


Figure 7. Graphite inclusions in sintered composites: №2 (a), №8 (b)

Graphite phase is distributed in the hard carbide-boride matrix nonhomogeneously (Fig. 7). Considerable amount of carbon is accumulated in 10 – 50µm areas mixed with TiB₂ particles (Fig. 6, 7), while rest of the phase forms isolated flake-like inclusions (Fig. 8).

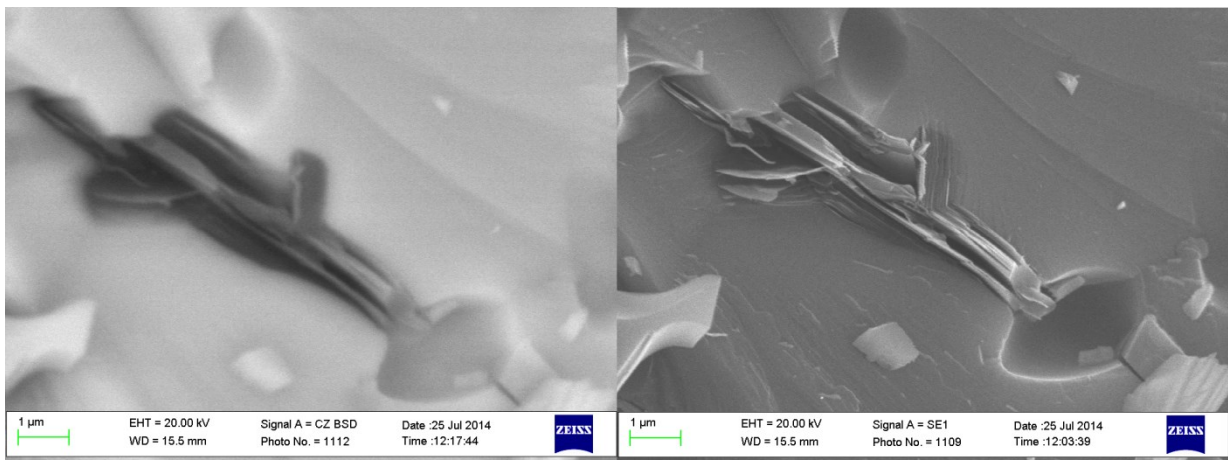


Figure 8. Flake-like graphite inclusion (sample 8)

Interestingly that additional milling of the initial powder mixture (it has been done for the stoichiometric sample 6) does not affect aforementioned graphite-enriched areas in the material after hot pressing so their appearance should also be referred to the composite sintering process.

3.3. Contactless TiC-B₄C interaction.

Following [13], boron carbide enthalpy reverses positive at temperatures higher than 1000°C thus it becomes unstable at elevated temperatures. As it can be seen from Table 3 data annealing of Fig.1 arrangement up to 1300°C doesn't alter surface phase composition significantly.

Table 3

Phase composition (according to XRD analysis) of B₄C and TiC sample surfaces (Fig. 7) after annealing

Annealing temperature	Surface phase composition, at%					
	TiC sample				B ₄ C sample	
	TiC	TiB ₂	TiCN	BN	B ₄ C	C (graphite)
1100 °C	100	-	-	-	97	3
1300 °C	100	-	-	-	95	5
1400 °C	94	2	4	-	66	34
1500 °C	57	33	10	-	62	38
1900 °C	23	52	23	3	58	42

At temperatures more than 1400°C titanium diboride formation occurred on TiC sample surface while boron carbide evidently decomposes losing boron atoms. Temperature increasing intensifies boron carbide decomposition resulting diboride being predominant phase on carbide sample surface. Thus the non-contact interaction experiment proved gaseous transport of boron atoms to be efficient way of TiB₂ creation at elevated temperatures.

3.4. Discussion. Interaction and structure formation mechanisms.

Correlation between consolidation and reaction stages according to densification kinetics and XRD data (Fig. 1 and 2) together with essential decreasing of sintering temperature and time comparing to similar material creation [16] allows to assume that the main role in presented composites structure formation plays the reaction (1) occurring alongside with hot pressing of initial powder mixtures. Sample sintering temperature ($\leq 1900^\circ\text{C}$) is considerably lower than melting points of both starting components and products hence the boron and titanium carbides interaction occurs with no liquid phase. As is shown in [17] titanium carbide has wide homogeneity region and actually is TiC_{1-x} where $x = 0.1 \div 0.4$ thus its cubic lattice contains a great amount of vacancies in carbon places which can easily be filled up with boron atoms being similar in their sizes to carbon ones. On the other hand, boron carbide formation enthalpy turns positive at 1000°C so B₄C phase becomes metastable at higher temperatures. Experiments in contactless TiC-B₄C interaction (See Fig. 1, Table 3) showed that its decomposition causes extremely effective boron atoms to TiC surface

transport at temperatures higher than 1400°C which correlates pointedly with the reaction (1) intensification (Fig. 2).

The solid-phase reaction between titanium and boron carbides most probably begins with B₄C decomposition. In TiC-B₄C contacts boron atoms diffuse into titanium carbide grains accumulating in vacant carbon places. At certain concentration the energy of solid solution of boron in TiC becomes higher than that of carbon in TiB₂ thus diboride nucleation occurs. The lattice tolerance to carbon decreases and provokes its migration towards grain boundary where it can dissolve in nearby carbide grain or (if there is lack of vacant places in the lattice) consolidate into plate-like precipitates (Fig. 8). New boride crystal appearing according to described mechanism should actually be a nucleus of oversaturated solid solution of carbon in titanium diboride. As is shown with EDX-analysis (Fig. 9) TiB₂ grains really contain approximately 10 at.% of C-atoms.

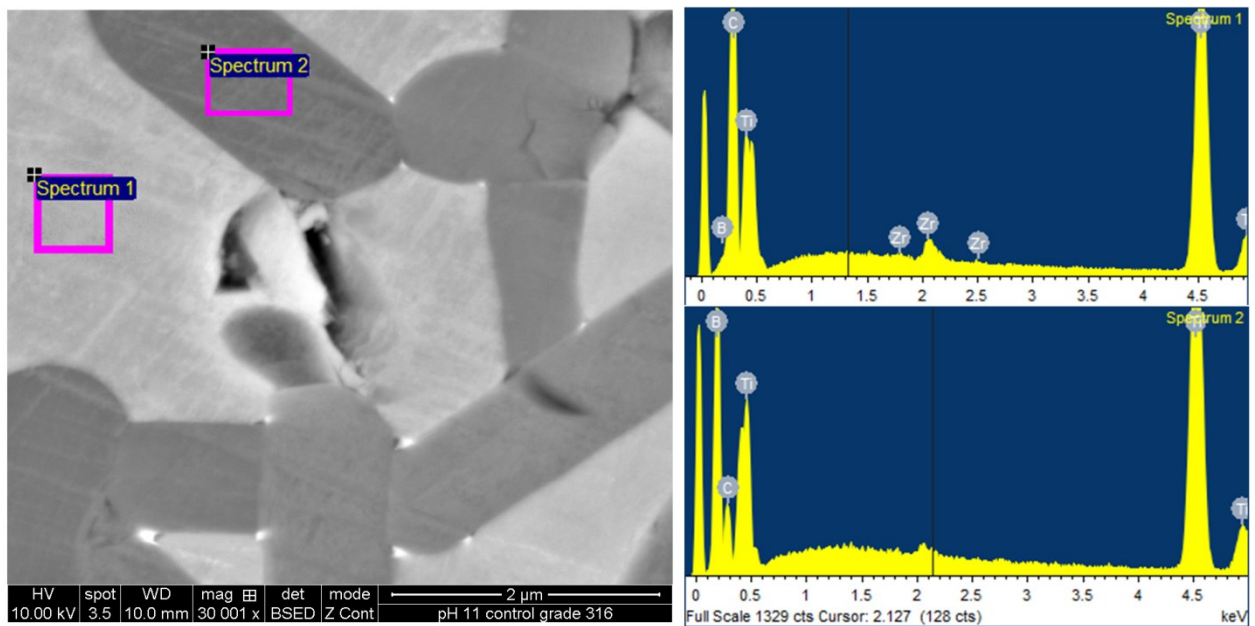


Figure 9. EDX analysis of sample 8 polished surface

The latter consequently means that considerable amount of carbon doesn't segregate into separate phase but remains inside diboride grains as solid solution. It means graphite (the most soft and light) phase content is approximately 20% less than estimated according to reaction (1). It should inevitably result density increasing which we indeed observed experimentally (See Table 2). It can be noted that considering [18], carbon solubility in titanium diboride is less than 2 at.% so aforementioned solid solution is in highly nonequilibrium state but, the investigation of the phase should be the topic of separate experimental work and here we just propose its appearance as the most probable explanation of all the collected data.

Thereby considering the reaction mechanisms and kinetics the first stage of composite structure formation begins at $T > 1000^{\circ}\text{C}$ with diffusion of boron into titanium carbide grains via intergranular contacts. After accumulating of B-atoms in certain volume of TiC grain TiB₂ nucleation occurs. Because of lattice discrepancy as well as probable carbon precipitation nucleated diboride nanoparticle breaks off the mother grain under external loading. Such destruction of grain contact regions initiates first densification stage and explains the presence of TiB₂ submicron particles (Fig.4). The reaction decelerates because of

product interlayer formation. Further temperature increasing results boron sublimation from all the surfaces of B_4C grains. B-atom transport via gas phase is not limited with titanium and boron carbides intergranular contacts. So the second consolidation wave begins. Reaction (1) heat effect increases almost linearly with temperature from $\Delta H \approx -170\text{kJ/mole}$ at 1000°C to $\Delta H \approx -220\text{kJ/mole}$ at 1800°C . Its adiabatic temperature at 1600°C amounts to 2600°C which is higher than boron carbide dissociation temperature (2450°C). Quick depletion of boron carbide surface provokes B diffusion from inner crystalline areas and formation of vacancies and vacancy clusters. Such clusters join into voids presented in Fig. 3a and 3b. When TiC amount is sufficient the depletion process can continue leaving at last shapeless carbon inclusion instead of B_4C grain. C-atoms being replaced with boron during TiC – TiB_2 transformation diffuse and cluster somewhere near nucleating diboride grain either piling up B_4C remnants or forming individual plate-like precipitates (Fig. 7). Such precipitates formation corresponds to John and Jenkins [19] referring to similar effect in annealed TiC-graphite system. When an amount of carbon is not sufficient to oversaturate nearby carbide lattice, clear TiC- TiB_2 interface (Fig. 9) appears.

Intensification of the interaction (1) at 1600°C increases temperature in local areas and accelerates titanium diboride and graphite formation. Graphite precipitates emerging into grain boundaries soften intergranular links. The latter occurring under the external pressure facilitates the densification and allows obtaining bulk heteromodulus refractory materials with improved toughness at comparatively low temperatures.

5. Conclusions

- Processes of the densification kinetics and structure of TiB_2 -TiC-C, TiB_2 -C and TiB_2 - B_4C -C heteromodulus ceramics produced via reaction hot-pressing of B_4C and TiC precursors are investigated.
- The interaction between titanium and boron carbides starts with B_4C decomposition and B-atoms accumulation inside TiC grains in vacant C places. At certain boron concentration initial TiC lattice ceased to possess the lowest energy and TiB_2 nucleus emerges pushing carbon out. Thus, two types of graphite areas in sintered composite structure can be described as (i) shapeless remnants of boron carbide and (ii) plate-like precipitates being formed as a result of TiB_2 nucleation.
- Titanium diboride produced during sintering contains approximately 10 at.% of carbon atoms failing to escape the lattice during TiC – TiB_2 transformation. In the result the soft graphite phase content in sintered composites is $\sim 20\%$ lower than the value which can be estimated basing on the reaction (1). The fact can explain higher density of created samples and should be considered in material composition prediction. material composition.
- The sintering of powder mixtures occur in two main stages. First stage begins at approximately 1100°C with boron atoms diffusion into TiC grains through intergranular contacts. The second is caused by

intense gaseous transport of boron atoms from B₄C grain surfaces occurring at temperatures higher than 1400°C and resulting in quick (16 minute at 1800°C) composite densification and reaction (1) completion.

References

1. Weimin Wang, Zhengyi Fu, Hao Wang and Runzhang Yuan: *J. Eur. Ceram. Soc.*, 2002, **22**, 1045–1049.
2. R. G. Munro: *J. Res. Natl. Inst. Stand.*, 2000, **105**(5), 709–720.
3. R. Koenigshofer, S. FuEernsinn, P. Steinkellner, W. Lengauer, R. Haas, K. Rabitsch and M. Scheerer: *Int. J. Refract. Met. Hard Mater.*, 2005, **23**, 350–357.
4. Hasselman, D. P. H., Becher, P. F. and Mazdiyasi, K. S., Analysis of the resistance of high-E, low-E brittle composites to failure by thermal shock. *Z. Werkstofftech.*, 1980, 11(3), 82–92.
5. Takafumi Kusunose, Tohru Sekino, Yong-Ho Choa, and Koichi Niihara. Machinability of Silicon Nitride/Boron Nitride Nanocomposites. *J. Am. Ceram. Soc.*, 85 [11] 2689–95 (2002)
6. D. P. H. Hasselman, *J. Am. Ceram. Soc.*, 53 (1970) 490.
7. D. P. H. Hasselman, P. T. B. Shaffer, WADD-TR-60-749, Part II (1962)
8. Lian Gao, Xihai Jin, Jingguo Li, Yaogang Li, Jing Sun. BN/Si₃N₄ nanocomposite with high strength and good machinability. *Materials Science and Engineering A* 415 (2006) 145–148
9. Xiuqing Li, Yimin Gao, Wu Pan, Xin Wang, Liancheng Song, Zhichao Zhong, Shanshan Wu. Fabrication and characterization of B₄C-based ceramic composites with different mass fractions of hexagonal boron nitride. *Ceramics International* 41(2015)27–36
10. I. L. Shabalin, Y. Wang, A. V. Krynkin, O. V. Umnova, V. M. Vishnyakov, L. I. Shabalin and V. K. Churkin: Physicomechanical properties of ultrahigh temperature heteromodulus ceramics based on group 4 transition metal carbides. *Advan. in Ap. Cer.*, 2010, Vol. 109,7, 405 – 415.
11. I. L. Shabalin, D. M. Tomkinson, and L. I. Shabalin, “High-temperature hot-pressing of titanium carbide – graphite hetero-modulus ceramics,” *J. Eur. Ceram. Soc.*, 27, No. 5, 2171–2181 (2007).

12. I. L. Shabalin. "Ridge effect" in oxidation kinetics of hetero-modulus ceramics based on titanium carbide. *Powder Metallurgy and Metal Ceramics*, Vol. 47, Nos. 1-2, 2008
13. NIST Chemistry WebBook: <http://webbook.nist.gov/chemistry/> 03/05/2013.
14. Tao Jiang, Zhihao Jin, Jianfeng Yang, Guanjun Qiao. Mechanical property and R-curve behavior of the B₄C/BN ceramics composites. *Materials Science and Engineering A* 494 (2008) 203 – 216.
15. O. Popov, V. Vishnyakov.
16. Weimin Wang, Zhengyi Fu, Hao Wang and Runzhang Yuan. Influence of hot pressing sintering temperature and time on microstructure and mechanical properties of TiB₂ ceramics: *J. Eur. Ceram. Soc.*, 2002, **22**, 1045–1049.
17. J. I. Murray: *Phase Diagrams of Binary Titanium Alloys*, (ASM, Metals Park, Ohio, 1987)
18. E. Rudy. "Ternary Phase Equilibria in Transition Metal-Boron-Carbon-Silicon Systems, Part V", Report # AFML-TR-65-2. Air Force Materials Laboratory, Wright-Patterson Air Force Base, OH, 1969.
19. D. John, G. M. Jenkins. Hot-working and strengthening in metal carbide-graphite composites. *Journal of Materials Science*, 21 (1986) 2941 – 2958